Satellite Remote Sensing of Groundwater: modeling, algorithm development and validation

Abduwasit Ghulam
(Institute of Remote Sensing and GIS, Peking University, Beijing, 100871, China)
abduwasit@yahoo.com
Qiming Qin
(Institute of Remote Sensing and GIS, Peking University, Beijing, 100871, China)
qmqin@pku.edu.cn

Abstract. Remote sensing has been widely used in the exploration of groundwater. In this paper, on the establishment of empirical function between ground water and soil moisture content 6S code is used to reduce uncertainties in the remote sensing of groundwater. Then ground water levels are calculated using 6S corrected and uncorrected ETM+ image along with isochronous meteorological information. Greater correspondence between field examined and satellite monitoring data is obtained from corrected image than from the uncorrected image.

Key words: remote sensing of groundwater, groundwater modeling

1. Introduction

With the development of remote sensing technology, multi-sensor data ranging from visible, infrared and microwave wavelengths is coming into widespread use in the remote estimation of groundwater[1-7]. However, the interaction of molecules and absorbing aerosols in the sun-sensor-target path generate negative effects on the quality of remotely sensed data, especially in the visible and infrared bands. As a result, to achieve accurate information on groundwater becomes difficult. The purpose of this study is the modeling and development of groundwater exploration algorithm using remote sensing as well as the validation of 6S atmospheric correction code in the reduction of uncertainties for groundwater monitoring. It is based on the Model of Groundwater Level Distribution in the Oasis and Desert Ecotone Using Remote Sensing (GLDRS), which is established with field examination surface data and laboratory analysis. Research area is the oasis and desert Ecotone (ODE) in Qira county, Xinjiang Uighur Autonomous Region of China (from E80º03′ ~ 82º10′to N35º17′ ~ 39º30′). The ODE is a special geographical space located between the oasis and desert, which is characterized with vegetation cover of 20%~30% and groundwater level of 2m~7m [7]. The climate of this area is an arid and semi-arid warm zone with annual rainfall averaging 34mm and an evaporation rate of 2595.3 mm.

2. Based image and its processing

Landsat ETM+ data was taken on 13 September 1999. After radiance pre-treatment and geometric correction, all the pixels represents for other classes except ODE were removed very carefully from ETM+ bands. 6S code used to eliminate atmospheric perturbation, here it is necessary to input parameters such as geometric parameters of the sensor, gases concentration, target elevation etc. We input the above parameters into 6S model to correct ETM+ image Band 2, 3, 4, and the output result is reflective radiation. Correction results show that spectrum brightness in band2 and 3 are increased. It is because of Rayleigh scattering and aerosols have a stronger effect on visible bands. Conversely, noticeable reduction is evident in band 4. This is acceptable since the contribution of vapor in the infrared channels is higher than the aerosol scattering. Due to the type of the surface which tends to increase the contrast between low and high reflective targets, the histograms of three channels are broadened.

3. The establishment of the GLDRS model for groundwater exploration

The soil moisture is mainly affected by the groundwater level since there is no irrigation and drainage in the ODE. When the groundwater level is situated near the surface, the superficial soil is supplied by capillary edge water and contains higher soil moisture. On the basis of stabilization of other factors, the soil spectrum is restricted distinctly by soil moisture. This can be expressed by an equation [8]:

$$R = a e^{bW} \qquad (1)$$

R is spectrum reflectivity, W is bulk moisture content, a, b regression coefficient.

Operating the formula (1) by logarithm, logarithm radix formation, statistical analysis and regressing on the field examined data in the research area, the following can be gained：

$$W_i = 65.0 - 42.9\lg(0.996B_i - 42.05) \qquad (2)$$

W_i is percent of soil moisture that is gained by ETM+ image ; B_i is spectrum radiation of corresponding band i .

The reflectivity of ETM+ image consists of two parts: vegetation radiation and soil radiation. In order to eliminate interference of vegetation to soil moisture, this paper introduces the concept of "optical vegetation cover", which is defined as the ratio of actual vegetation optical information to the information when the whole research area is covered with vegetation. The optical vegetation cover of per pixel is estimated by the spectrum radiance of 2、3、4 band[8,9]. In order to eliminate the interference of vegetation, the compound pixel spectrum information is translated into bare-soil spectrum luminosity and reflectivity R_{4i} . The conversion formula is defined as using band 4:

$$R_{4i} = \frac{0.6968B_2+0.5228B_3-0.2237B_4+18.76}{1.089-0.00579B_4+0.003308B_2+0.002482B_3}-42.05 \qquad (3)$$

Replacing with formula (2), Formula (3) can be changed into:

$$W_4 = 65.0-42.91\lg\left(\frac{0.6968B_2+0.5228B_3-0.2237B_4+20.26}{1.089-0.00579B_4+0.003308B_2+0.002482B_3}-18.0\right) \qquad (4)$$

The physical basis of remote determination of groundwater level is the existence of capillary edge in the soil layer over groundwater level, and the rising of groundwater to the surface through capillary edge.

Supposing that y is the vertical coordinate axis, and $y = 0$ means the interface of soil and air, the water distribution within capillary edge is described as follows[9]：

$$W^2(y) = A + By,\ \max(0, H - H_m) \le y \le H_m \qquad (5)$$

H is the depth of groundwater occurrence, H_m is the height of rising of the capillary edge in the soil half-space above the soil-water interface.

Using boundary conditions of groundwater and surface, the relationship between soil moisture and groundwater level is found to be：

$$H_{ETM+} = d + H_m \times \frac{W_{max}^2-\left[65.0-42.91\lg\left(\frac{0.6968B_2+0.5228B_3-0.2237B_4+20.26}{1.089-0.00579B_4+0.003308B_2+0.002482B_3}-18.0\right)\right]^2}{W_{max}^2+W_{min}^2} \qquad (6)$$

W_{max} , W_{min} denote maximum and minimum moisture capacity.

4. Application and feasibility analysis

$W_{max} = 35\%$， $W_{min} = 3.28\%$， $H_m = 6.3m$ is measured through field survey and laboratory analysis. Applying the above parameters and the effective depth of soil moisture measured by EMT+ to formula (7), groundwater level is computed and estimated by using 6S corrected and uncorrected images respectively. Thematic maps of groundwater level distribution (GWLD) are made with groundwater level classification of 1m≤ H <3m , 3m≤ H <5m, 5m≤ H ≤7m, see fig. 1.

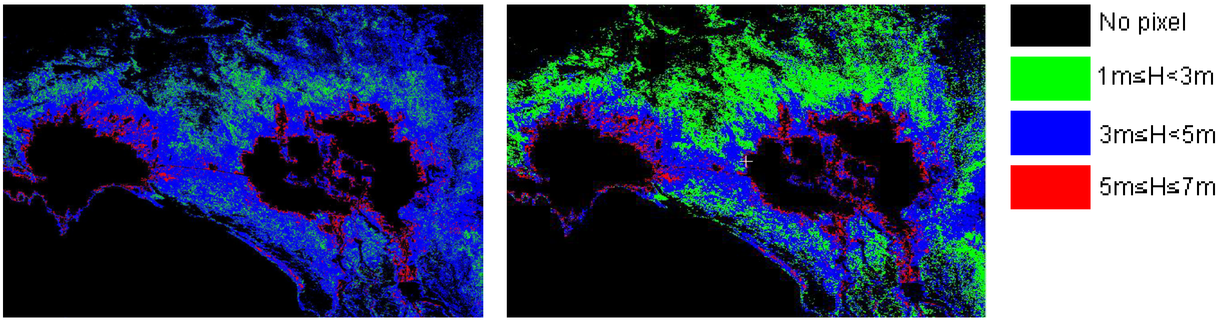

Fig. 1 Groundwater level distribution (GWLD) map of oasis and desert Ecotone. (On the left picture, GWLD is evaluated using ETM+ image without 6s atmospheric correction; on the right, 6S atmospheric data corrected image is used to evaluate GWLD).

Evaluation results show that the GLD achieved by GLDRS model in ODE is identical with terrain conditions of the research region and the practical status of groundwater level distribution in this area. There is obvious improvement in the correlation and accuracy of remote monitored groundwater levels after 6S correction. Correlation coefficient of theoretical and practical groundwater level is 0.83 for the uncorrected image and 0.94 for the corrected one.

5 Conclusion

This paper uses the 6S model to eliminate the coupled effect of atmosphere and land surface and to improve the performance of GLDRS model. Aerosols and vapor resulted in errors when surveying groundwater level. The paper concludes that in arid and semi-arid regions, it is feasible to use GLDRS to estimate groundwater level. 6S atmospheric simulation model eliminates effectively the perturbation from geometric and system corrected Landsat ETM+ imagery.

Acknowledgements

This paper was supported by the Hi-Tech Research and Development program of China (Grant No.2 001AA135110).

References

[1] J.M. Whiting. Airborne Thermal Infra-red Sensing of Soil Moisture and Groundwater [A]. Remote Sensing of Soil Moisture and Groundwater [C]. CANADA, 1976.

[2] A.A. Omar. Use of SIR-A Interpretation for Underground Water Prospecting in Southern Iraq [A]. Remote Sensing: an Operational Technology for the Mining and Petroleum Industries[C]. 1990:165~172

[3] Debasish Das. Extraction of Geomorphic and Geologic Information for Groundwater Exploration through Satellite Remote Sensing In and Around the WICHITA Mountains, OKLAHOMA [A]. Eighth Thematic Conference on Geologic Remote Sensing [C]. 1991, 1:171~180.

[4] K.R. Knapp, K.M. Morgan. Using SPOT and TM to Map Fractures Related to Ground-Water Resources in the Slick Hills of Oklahoma [A]. Tenth Thematic Conference on Geologic Remote Sensing [C]. 1994, 1:155~167.

[5] J. KRISHNAMURTHY , G. SRINIVAS. Role of Geological and Geomorphological Factors in Ground Water Exploration: A Study Using IRS LISS Data [J]. International Journal of Remote Sensing, 1995, 16（14）：2595~2618.

[6] J.W. Finch. Location of High Yielding Groundwater Sites in Zimbabwe Use of Remote Sensed Data [A]. Remote Sensing: an Operational Technology for the Mining and Petroleum Industries[C]. 1990:147~152.

[7] Tashpolat Tiyip, Abduwasit Ghulam. Research on the Model of Groundwater level Distribution in the Oasis and Desert Ecotone Using Remote Sensing [J]. Journal of Remote Sensing, 2002, 6（4）：299~306.

[8] Liu Peijun, Zhang Lin, Alishir Kurban, Chang Ping. A Method for Monitoring Soil Water Contents Using Satellite Remote Sensing [J]. Journal of Remote Sensing, 1997, 1(2): 135~138.

[9] S.A Komarov, V.L. Mironov, A.N. Romanov, A.V. Yevtyushkin. Remote Sensing of Water Table: Measurement and Data Processing Algorithm [J]. Mapping Science and Remote Sensing, 1999, 36(1): 1~10.